Molecular Biology of the Cell
Vol. 19, 5006–5018, November 2008

Retrograde Flow and Myosin II Activity within the Leading Cell Edge Deliver F-Actin to the Lamella to Seed the Formation of Graded Polarity Actomyosin II Filament Bundles in Migrating Fibroblasts

Tom W. Anderson,* Andrew N. Vaughan,* and Louise P. Cramer*†

*MRC-Laboratory Molecular Cell Biology, and †Department of Cell and Developmental Biology, Faculty of Life Science, University College London, London WC1E 6BT, United Kingdom

Submitted January 16, 2008; Revised July 28, 2008; Accepted September 5, 2008
Monitoring Editor: Paul Forscher

In migrating fibroblasts actomyosin II bundles are graded polarity (GP) bundles, a distinct organization to stress fibers. GP bundles are important for powering cell migration, yet have an unknown mechanism of formation. Electron microscopy and the fate of photobleached marks show actin filaments undergoing retrograde flow in filopodia, and the lamellipodium are structurally and dynamically linked with stationary GP bundles within the lamella. An individual filopodium initially protrudes, but then becomes separated from the tip of the lamellipodium and seeds the formation of a new GP bundle within the lamella. In individual live cells expressing both GFP-myosin II and RFP-actin, myosin II puncta localize to the base of an individual filopodium an average 28 s before the filopodium seeds the formation of a new GP bundle. Associated myosin II is stationary with respect to the substratum in new GP bundles. Inhibition of myosin II motor activity in live cells blocks appearance of new GP bundles in the lamella, without inhibition of cell protrusion in the same timescale. We conclude retrograde F-actin flow and myosin II activity within the leading cell edge delivers F-actin to the lamella to seed the formation of new GP bundles.

INTRODUCTION

Cell migration is essential for embryo development, tissue repair, and immunity in both the embryo and the adult and plays an important role in several diseases. Cell migration is driven by motile forces generated by several distinct types of actin filament structures in cells, and an understanding of their formation is thus essential to advance knowledge on cell migration mechanisms. It is thought that several distinct actin force generating mechanisms in a single cell together provide overall force for cell migration: actin filament assembly is coupled to membrane protrusion at the leading cell edge, whereas actin filaments and myosin II and possibly other types of myosins in the cell body contribute motile force in the form of cell tension to drive the cell body and cell rear forward (collectively termed here for simplicity cell body translocation; reviewed in Sheetz, 1994; Lauffenburger and Horwitz, 1996; Mitchison and Cramer, 1996; Cramer, 1999a; Sheetz *et al.*, 1999; Verkhovsky *et al.*, 1999; Small and Resch, 2005).

Formation of protrusive structures (lamellipodia and filopodia) at the leading edge of migrating cells has been extensively studied, and much progress in determining the molecular mechanism of their formation has been made in recent years (reviewed in Small, 1995; Pollard and Borisy, 2003; Ridley *et al.*, 2003; Faix and Rottner, 2006; Carlier and Pantaloni, 2007; Gupton and Gertler, 2007; Mattila and Lappalainen, 2008). Filopodia are embedded within, or protrude from, the lamellipodium and are thought to mainly have a role in directionality (reviewed in Faix and Rottner, 2006; Gupton and Gertler, 2007; Mattila and Lappalainen, 2008). Length of individual filopodia may vary such that its tip is located either at the front edge of the lamellipodium, as seen in chick embryo fibroblasts (e.g., Figure 1b, open arrowheads) or some distance beyond it, as, for example, is more typical in neurite growth cones.

Actin in the cell body has been less extensively studied, despite its importance for cell migration. Almost all information on actin in the cell body comes from the study of stress fibers, a type of actomyosin II filament bundle (Badley *et al.*, 1980; Pellegrin and Mellor, 2007). However although this information is useful in some contexts, not yet widely appreciated is that actin in the cell body in migrating cells is not organized as stress fibers. Currently, the only way to identify actin organization and filament polarity is by electron microscopy (EM) and decorating the filaments with subfragments of myosin II. Where this has been done in migrating cell types, actin organization is distinct to stress fibers (Cramer *et al.*, 1997; Svitkina *et al.*, 1997; Swailes *et al.*, 2004). Although stress fibers are organized with alternating filament polarity, similar to muscle sarcomeres (Cramer *et al.*, 1997; Cramer, 1999a), actin organization in migrating cells is distinct, either graded filament polarity in migrating fibroblasts (Cramer *et al.*, 1997) and migrating myoblasts (Swailes *et al.*, 2004) or a distinct nonsarcomeric actomyosin II filament network in migrating keratocytes (Svitkina *et al.*, 1997). Further, the formation of stress fibers is associated with reduced cell movement (Couchman and Rees, 1979).

This article was published online ahead of print in *MBC in Press* (http://www.molbiolcell.org/cgi/doi/10.1091/mbc.E08–01–0034) on September 17, 2008.

Address correspondence to: Louise P. Cramer (l.cramer@ucl.ac.uk).

Abbreviations used: GP, graded polarity.

There are two important, yet not fully appreciated, consequences for the different underlying actin organizations identified in the cell body of migrating cell types and stress fibers in other cell types (Cramer, 1999a; Verkhovsky *et al.*, 1999). One is that their mechanisms of formation must be distinct. Another is that the mechanism of myosin II force generation in the cell body of these migrating cells must be distinct to cell tension generated in stress fibers, clearly having a consequence for the mechanism of cell migration. As we want to understand how cells move, here we have thus studied how graded polarity actin filament bundles form in migrating primary chick embryo heart fibroblasts.

Migrating, primary chick heart fibroblasts and migrating mouse myoblasts are the only migrating cell types in which actin organization and filament polarity is completely known throughout the entire cell, thus making them excellent models for developing an understanding of how cells move. In both cases actin is organized with graded filament polarity (GP), either actin bundles in migrating fibroblasts (Cramer *et al.*, 1997) or actin sheets in migrating myoblasts (Swailes *et al.*, 2004). Thus graded polarity is an important actin organization for cell migration.

Migrating primary chick fibroblasts are composed of several distinct cell regions distinguished by morphology (see Figure 1) and behavior and actin dynamics (Cramer *et al.*, 1997). At the front of the cell is the leading cell edge, rich in polymerized (F-) actin. The leading cell edge in these cells comprises a lamellipodium (Figure 1a, denoted lp) and filopodia (Figure 1b, open arrowheads) embedded within the lamellipodium. Immediately behind the lamellipodium is a region termed the lamella (Figure 1a, denoted la), of intermediate thickness and comprised of less rich F-actin (Cramer *et al.*, 2002). Behind the lamella, is the bulk cell body, containing the nucleus and most of the organelles (Figure 1a, denoted n). Behind the nucleus is a rounded, or drawn-out cell rear (Figure 1a, denoted r). For clarity, in this article the term leading cell edge is used to refer to both the lamellipodium and filopodia embedded within individual lamellipodia. Also in this article the boundary between the lamellipodium and lamella is also studied (Figure 1a, dashed line). This boundary in fibroblasts is readily distinguished based on the known differences in morphology by phase-contrast or DIC microscopy (Heath and Holifield, 1991) and that F-actin concentration is higher within the lamellipodium (Cramer *et al.*, 2002; see also Figure 1a, compare lp and la at their boundary; dashed line).

In these migrating fibroblasts, F-actin dynamics with respect to the substratum varies with spatial location in the same cell (Cramer *et al.*, 1997). In the lamellipodium and filopodia F-actin flows retrograde (backward). Within the lamella F-actin is stationary, and within the bulk cell body there are two dynamic F-actin populations, one population flows anterograde (forward) and the other is stationary. Other migrating cell types also exhibit retrograde, anterograde, and stationary F-actin dynamic behavior within the same individual cell (Svitkina *et al.*, 1997; Salmon *et al.*, 2002; Vallotton *et al.*, 2004; Schaub *et al.*, 2007), although the precise spatial cellular location of each actin dynamic varies with cell type. In the context of this article, we point out that observed stationary behavior of F-actin with respect to the substratum within the lamella of migrating fibroblasts (Cramer *et al.*, 1997) contrasts to observed slow retrograde F-actin flow in the lamella of some other motile cells (Salmon *et al.*, 2002; Vallotton *et al.*, 2004) or lamella-equivalent regions in some type of neuronal growth cones (Forscher and Smith, 1990; Schaefer *et al.*, 2002). This difference may reflect precise cell behavior (Verkhovsky *et al.*, 1999). For the forward flow and stationary actin populations in migrating cells evidence provides a role in driving the cell body forward during migration (Cramer *et al.*, 1997; Cramer, 1999a). Retrograde F-actin flow has been studied for decades and seems a common behavior in motile cells (Cramer, 1997; Vallotton *et al.*, 2005). In some migrating cell types there is a relationship between the rates of retrograde F-actin flow and leading edge protrusion (Lin and Forscher, 1995; Mallavarapu and Mitchison, 1999; Giannone *et al.*, 2004). However, additional explicit functions for retrograde F-actin flow is less explored in the literature.

GP actin filament bundles in migrating fibroblasts span the entire cell, apparently from the front of the lamella (Figure 1a, GP bundles indicated with solid arrowheads) to the rear cell margin, and their dynamic behavior is determined by position in the cell: stationary within the lamella and stationary and forward moving within the bulk cell body (Cramer *et al.*, 1997). GP actin filament bundles are predominantly oriented in the direction of migration and are mostly localized on the ventral cell surface where they are associated with adhesion proteins such as talin (Cramer *et al.*, 1997). GP bundles provide the myosin II–based motile force needed to move the bulk cell body forward during cell migration (Cramer *et al.*, 1997, 1999a). Despite their importance for cell migration, the mechanism of formation of GP bundles is unknown.

We have found that a subpopulation of F-actin within filopodia, and the lamellipodium is delivered to the lamella by retrograde F-actin flow and myosin II activity to seed the formation of new GP actin filament bundles in this location. For the first time this provides information on the mechanism of formation of GP actin filament bundles as well as providing an explicit function for retrograde actin filament flow in cells. Our data also provides direct evidence for a new actin assembly pathway where actin filaments in filopodia and lamellipodia directly supply actin filaments to seed construction of actomyosin II bundles in the lamella. Thus protrusion of the leading cell edge and retrograde F-actin flow is structurally and dynamically coupled with tension-generating activity within GP bundles in the cell body to provide necessary overall coordination in motile forces to move the entire cell forward.

MATERIALS AND METHODS

Preparation of Primary Chick Embryo Fibroblasts

Hearts were dissected from 7-d-old chick embryos and mechanical preparation of tissue explants were plated on coverslips coated with poly-L-lysine and Matrigel (BD Biosciences, San Jose, CA) and cultured in DMEM, high-glucose (Invitrogen, Paisley, United Kingdom), with 10% calf serum (Invitrogen), 10% chick serum (Sigma, St. Louis, MO), and 100 U/ml each of penicillin and streptomycin (Sigma). As previously described (Cramer, 1999b), once the explant had adhered, fibroblasts moved out, and migrating cells at the periphery of the halo of the explant 18–30 h after plating were used for study. These cells at this time migrated at 0.5–2 um/min.

Electron Microscopy

Cells grown on glass coverslips coated with poly-L-lysine and Matrigel were permeabilized live in cytoskeleton buffer (10 mM MES, pH 6.1, 2 mM $MgCl_2$, 2 mM EGTA, 138 mM KCl, and 380 mM sucrose) containing 1% Triton X-100 and 1 μg/ml unlabeled phalloidin for 10 min. We titrated the time and concentration of detergent necessary to obtain the minimal dose required to provide good visualization and preservation of actin filaments at the front of the cell. Cells were then fixed in 4% glutaraldehyde in 0.1 M sodium cacodylate buffer, pH 7.6, and postfixed in 1% osmium tetroxide/1.5% potassium ferricyanide, and then were prepared for whole mount EM, critical point drying, platinum and carbon coating, and rotary shadowing as previously described, except that the digestion step with 10 M NaOH was done if required (Signoret *et al.*, 2005). In this method, the coating with platinum and carbon was thick (~2 × 10–14 nm).

Construction of EGFP-tagged Myosin Essential Light Chain

A clone of the chicken nonmuscle myosin essential light-chain cDNA (GenBank entry no. M15646) was a kind gift from K. Trybus (University of Vermont). Enhanced green fluorescent protein (EGFP) was fused to the N terminus by cloning the full myosin light-chain coding sequence into pEGFP-C1 (Clontech, Mountain View, CA), such that there was a 37-aa linker between the two. Sequencing of the myosin light-chain clone revealed a point mutation that results in a K66N mutation in the protein. This residue is not conserved across the vertebrates, and this substitution is found in the corresponding sequence in turkey (*Meleagris gallopavo*). The EGFP-tagged myosin essential light-chain (EGFP-ELC) viral (see below) construct showed complete colocalization with endogenous myosin II when expressed in chick embryo fibroblasts (CEFs) (Supplementary Figure S1). At moderate expression levels actin organization and cell behavior was the same as uninfected cells. Highly expressing cells were not used for analysis because cell shape appeared more amorphous. Thus at moderate expression levels this construct is a faithful reporter of myosin II localization and cell behavior.

Preparation and Use of Adenovirus Suspensions

The AdEasy system (Stratagene, La Jolla, CA) was used to produce recombinant, E1- and E3-deleted adenoviruses of EGFP-ELC myosin II, EGFP-actin (Tanner *et al.*, 2005), and mRFP-actin. EGFP-actin and mRFP-actin viruses were a kind gift from J. Bamburg (Colorado State University). Viruses were made, expanded, and titered as described (Minamide *et al.*, 2003). In brief, viruses were produced and amplified by infecting HEK 293 cells with viral constructs, collecting the supernatant 2 to 3 d later, and concentrating by centrifugation on a 100-kDa molecular-weight cutoff ultrafilter (Millipore, Billerica, MA). Viral stocks were titrated by infecting confluent HEK 293 cells with serial dilutions of the stock, fixed 16 h later, stained with the B6-8 anti-E2a antibody, and counted infected cells. CEFs were infected by incubating fresh explants held in suspension with doses of 10^7 U in 100 μl per heart for 24 h before plating, similar to previous studies (Dawe *et al.*, 2003). As described previously (Dawe *et al.*, 2003), where two distinct viral constructs were used to infect a single population of cells (as in Figure 6), the proportion of each virus had to be reduced to ensure most cells remained healthy. This meant that in healthy cells the intensity of the signal for GFP-myosin II and RFP-actin in a dual infection and expression was less than in a single infection.

Live Imaging of Cells

Cells expressing GFP-actin or RFP-actin, or coexpressing GFP-myosin II and RFP-actin were cultured on glass-bottomed dishes (Willco Wells, Amsterdam, Netherlands) coated with Matrigel in phenol red–free DMEM/F12 (Invitrogen) supplemented as above, and imaged for total fluorescence or for photobleaching experiments. For total fluorescence (see Figures 3, b, c, and i, 6, and 7), cells were imaged live every 10–15 s at 37°C with a system comprising an Eclipse TE-2000U inverted microscope body with a 60× objective (Nikon Instruments, Kawasaki, Japan), a CSU-10 spinning disk confocal scanner (Yokogawa Electric, Tokyo, Japan) and an Orca IIER digital camera (Hamamatsu Photonics, Hamamatsu City, Japan), controlled by Metamorph 5 software (Molecular Devices, Sunnyvale, CA). For photobleaching experiments (see Figures 2 and 4) and for higher temporal resolution imaging without photobleaching (Figure 3g), cells expressing GFP-actin were imaged live every 1 s at 37°C with a 60× objective on a Leica SP5 confocal microscope (Deerfield, IL). For photobleaching the Leica photobleaching module software was used.

Cell Staining for Light Microscopy

Cells were fixed with either 4% methanol-free formaldehyde (TAAB, Aldermaston, United Kingdom) in cytoskeleton buffer (10 mM MES pH 6.1, 2 mM $MgCl_2$, 2 mM EGTA, 138 mM KCl, 380 mM sucrose) at 37°C for 10 min, or ice-cold methanol at room temperature for 3 min. Fixed cells were permeabilized with 0.5% Triton X-100 for 10 min, blocked with 2% BSA, and labeled with fluorophore-conjugated phalloidin and Hoechst 33342, and indirect immunofluorescence was performed. Antibodies used were as follows: C4 anti-actin (MP Biomedicals, Solon, OH); A2066 anti-actin, and 6490-1004 anti-myosin II (Biogenesis, Poole, United Kingdom). Stained cells were imaged at 60× or 100× using an Eclipse E-800 microscope (Nikon Instruments) equipped with a SenSys camera (Photometrics, Tucson, AZ).

RESULTS

Actin Filaments within GP Bundles Are Contiguous with Actin Filaments in Filopodia and the Lamellipodium in Migrating Cells

As previously recognized GP bundles appear to extend to the front of the lamella in migrating fibroblasts (Cramer *et al.*, 1997; Figure 1, a and b). We further assessed and tested this in more spatial detail by whole mount EM. By EM, actin filaments within each GP actin bundle visualized at the front of the lamella is clearly contiguous with either actin filaments within the rear of a filopodium (Figure 1, c and e) or within the rear of a subzone of the lamellipodium (Figure 1, d and f), supporting the light microscopy observations (Figure 1, a and b). Tracing individual actin filaments deeper in the leading cell edge was not possible because of the density of actin filaments in this region. Quantification (Figure 1g) shows that individual actin filaments within an average 95.1% of GP bundles in the cell population (ranging 88.9–100% in individual cells) are contiguous with actin filaments within the leading cell edge: 51.6% within filopodia and 43.5% within the lamellipodium. Thus actin filaments within GP bundles at the front of the cell are structurally contiguous with actin filaments within the lamellipodium and filopodia.

Retrograde Flow of a Proportion of Actin Filaments Originating within the Leading Cell Edge Is Delivered to the Lamella and Then Stops Moving

As previously described, actin filaments flow retrograde (rearwards) in the lamellipodium, yet are stationary with respect to the substratum in the lamella in migrating chick embryo fibroblasts (Cramer *et al.*, 1997). In this previous analysis, marks were made on actin filaments separately, either within the lamellipodium or lamella, respectively, and their behavior assessed only within that zone. To test whether there is a dynamic link between these two spatial actin populations, in live cells expressing a fusion protein of GFP-actin, we photobleached marks on GFP-actin filaments within the lamellipodium and filopodia embedded within the lamellipodium and assessed the fate of the bleached zone (Figure 2; see also Supplemental Movie S1). As expected, the bleached mark flowed retrograde with respect to the substratum. However, although actin subunits within the mark also turned over, also as expected, fluorescence recovery was incomplete and a subpopulation of F-actin continued flowing into the lamella. Here, the bleached zone apparently stopped moving with respect to the substratum as far as we could detect and measure (Figure 2, compare a–e with the kymograph in f). This occurred in 100% (31/31) cases where the same individual zone originally bleached in the lamellipodium and filopodia was then also resolvable in the lamella. This represented 88.6% (31/35) total cases (Figure 2g). In a further 11.4% minority (four cases) the bleached zone flowed to the lamella, but was then not clearly resolvable to assess dynamics. In a further two cases, the bleached zone fully recovered fluorescence within the lamellipodium and filopodia. The precise spatial location where the conversion from moving to stationary actin dynamics occurs is apparently at the boundary of the lamellipodium with the lamella, as the rear of photobleached marks made within this region did not move retrograde. Thus in the majority of cells, a proportion of actin filaments that originate within the lamellipodium and filopodia are relocated by retrograde flow to the front of the lamella, where the same marked filaments then become stationary with respect to the substratum.

We then specifically addressed the dynamic relationship between F-actin within the leading cell edge and GP bundles within the lamella. This was more difficult and analysis was limited because of the combination of the inherent small size of any mark made within individual filopodia, partial recovery of fluorescence during retrograde flow of the mark before reaching the lamella, and that the concentration of F-actin is weaker within the lamella than within the lamellipodium (Cramer *et al.*, 2002). However in 35% (11/31)

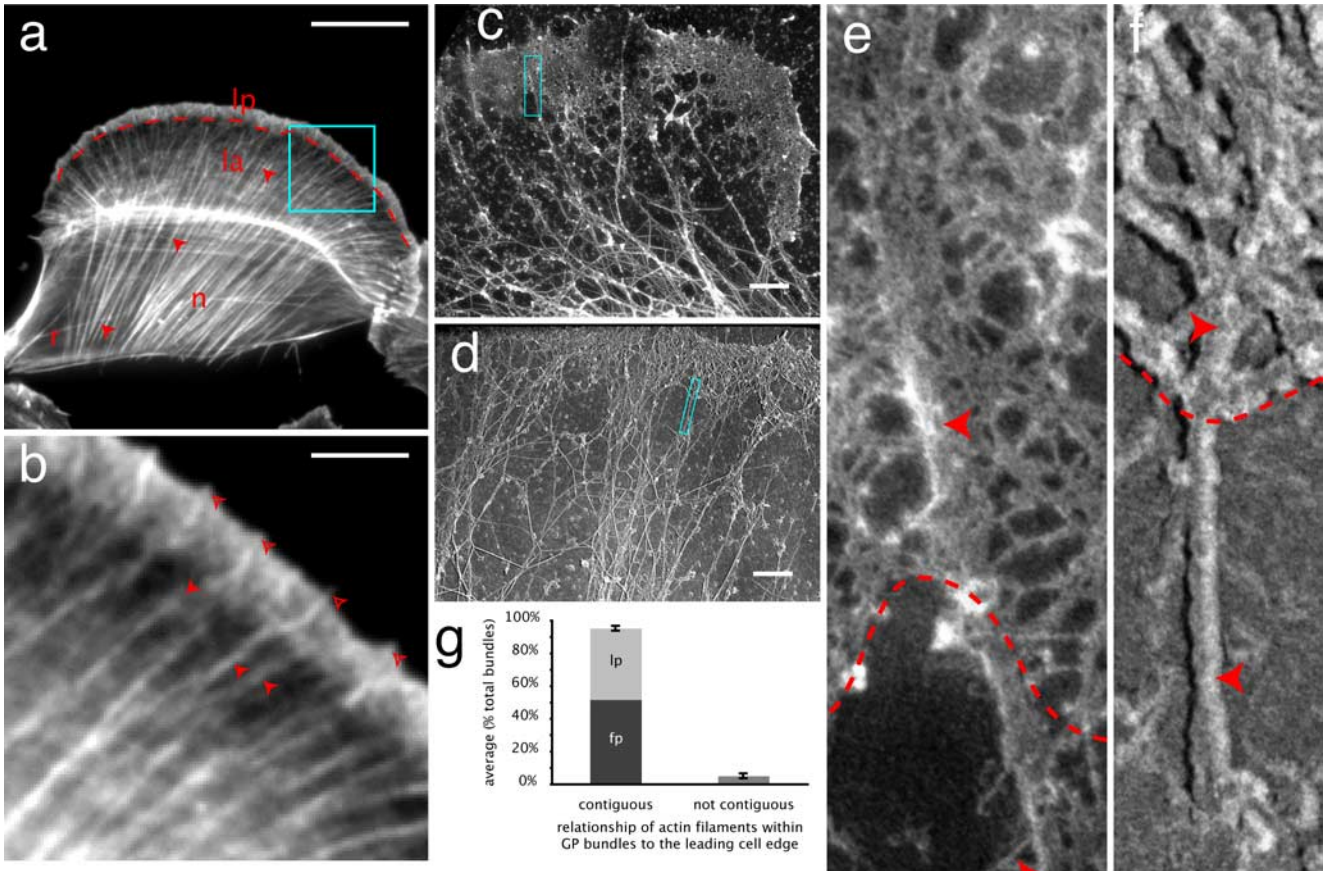

Figure 1. Actin filaments within the leading cell edge and GP bundles are structurally contiguous. (a and b) A migrating chick embryo fibroblast fixed and stained for F-actin with Alexa 594-phalloidin. (a) Labels indicate the lamellipodium (lp), lamella (la), nuclear region (n), and cell rear (r). A dashed line indicates the boundary between the lamellipodium and lamella. Solid arrowheads indicate GP bundles. (b) An enlarged view of the box region in panel a shows the region of the lamellipodium and the front part of the lamella in more detail. Hollow arrowheads indicate filopodia embedded within the lamellipodium, and solid arrowheads indicate GP actin filament bundles at the front of the lamella. (c–g) Whole mount EM images (c–f) of the front of the cell in two (c, e and d, f) migrating fibroblasts. The GP bundle in the boxed region (c and d) is located at the lamellipodium–lamella boundary. (e and f) Enlarged views of the boxed regions in c and d, respectively; the boundary between the lamellipodium and lamella is indicated with a dashed red line, and an actin filament from the tip of a GP bundle in the lamella (lower red arrowhead) is contiguous with the actin filament (upper red arrowhead) within a filopodium (e) or lamellipodium (f). (g) Quantification of tracing the spatial location of actin filaments within the ends of GP bundles visualized in EM images (average, n = 230 GP bundle ends in seven cells). Lp denotes contiguous with F-actin within the lamellipodium, and fp denotes contiguous with F-actin within a filopodium. Variation in appearance of the two different cells in c and d is due to slight difference in the critical point drying. Apparent actin filament width is increased due to platinum and carbon coating (see *Materials and Methods*). Bars, (a) 18 μm, (b) 3 μm, (c and d) 1 μm, and (e and f) 100 nm.

cases the signal-to-noise was sufficient. In all 11/11 cases, bleached marks originally made on GFP-actin filaments within filopodia (Figure 2i) or within regions in the lamellipodium were subsequently relocated to GP bundles at the front of the lamella (Figure 2k; see also Supplemental Movie S2). These results demonstrate that actin filaments within filopodia and the lamellipodium are dynamically linked with GP actin filament bundles in the lamella.

F-Actin within Filopodia and Subzones within the Lamellipodium Seed the Formation of New GP Bundles within the Lamella in Migrating Cells

The observed structural (Figure 1) and dynamic (Figure 2) link between actin filaments in filopodia, the lamellipodium, and GP bundles infers that GP bundles are formed at least in part using actin filaments from the leading cell edge. To further test this, we determined in a separate body of experiments from prelife history analysis in live migrating fibroblasts expressing GFP-actin that 95% of newly formed GP actin filament bundles were derived from the leading cell edge and a further 5% apparently directly from within the lamella. In further spatial analysis of only the leading cell edge, 80% of new GP bundles were derived from filopodia and 20% apparently from subzones within the lamellipodium (Figure 3a).

For the population of GP bundles derived from filopodia, detailed analysis (see also Supplementary Movies S3 and S4) reveals that an individual filopodium initially protrudes (Figure 3c, compare hollow arrowheads, −50 to −10 s), but then ceases net protrusion, whereas that of the lamellipo-

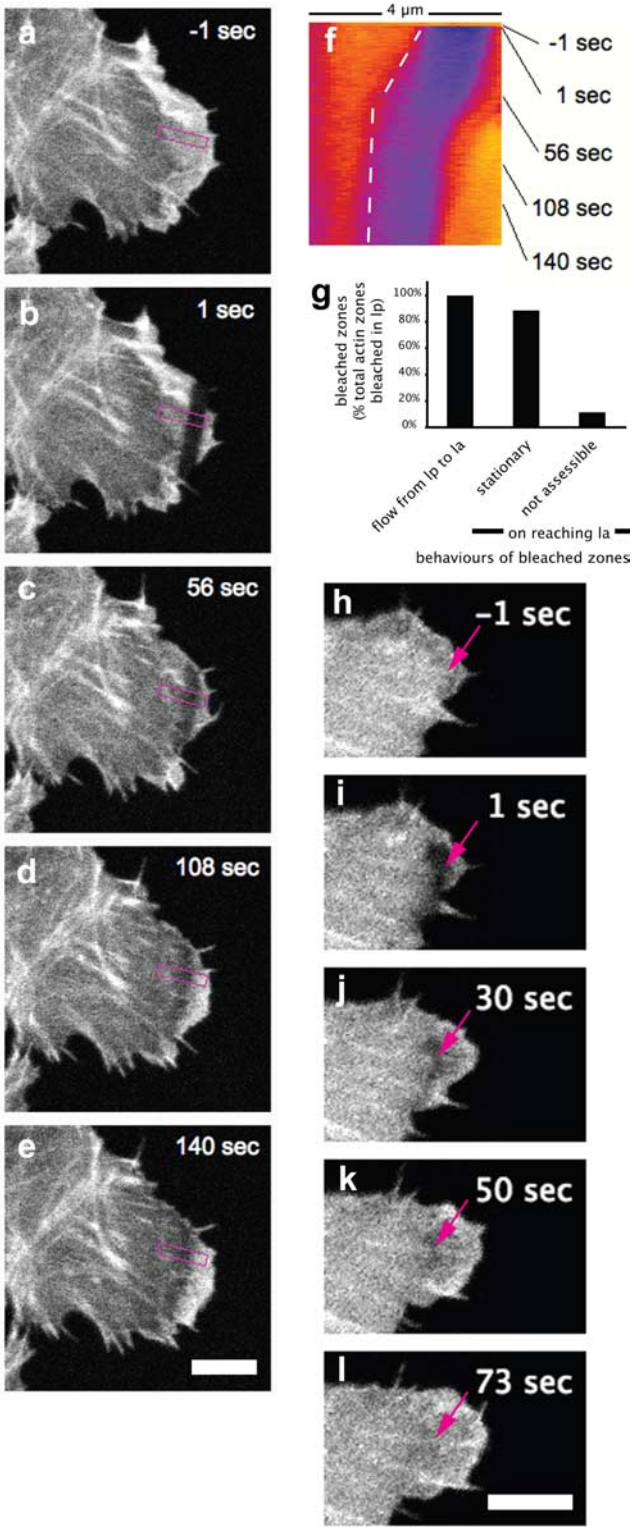

Figure 2. Actin filaments within the leading cell edge and lamella are dynamically linked. Live cells expressing GFP-actin were imaged every 1 s with a SP5 confocal microscope, and a subzone within the leading cell edge was photobleached and then tracked. (a–e) Retrograde F-actin flow (rate in this lamellipodium is 0.64 um/min) with respect to the substratum occurs through the lamellipodium (b and c, dark band moves leftwards in the box), reaches the boundary with the lamella (c and d), and stops flowing within the lamella (d and e, no movement leftwards at the rear of the mark). (f) Kymograph (4 μm across) of the box region in a–e. Diagonal dashed line shows retrograde F-actin flow within the lamellipodium, and vertical dashed line shows no flow within the lamella. Gray scale value intensities were colored with a cool hue look up table in ImageJ (http://rsb.info.nih.gov/ij/). The photobleached zone appears purple/blue. (g) Quantification of behavior of the zone originally bleached within the lamellipodium and tracked to the lamella (n = 35 bleached zones in 19 live cells). (h–l) Leading cell edge and lamella of a different cell: a filopodium is indicated with an arrow (h), a zone on the filopodium is photobleached (i) and tracked (i–k), and the bleached zone is then visible within a GP bundle in the lamella (k) that recovers by panel l. Bars, (e and l) 5 μm.

dium continues. The filopodium tip thus becomes separated from the tip of the bulk lamellipodium (e.g., Figure 3c, solid arrowhead, 0 s). Once the filopodium is separated, in contrast to protruding filopodia, the tip of the separated filopodium remains net stationary with respect to the substratum (Figure 3c, compare solid arrowheads, 0–100 s). Because this actin structure is no longer undergoing net protrusion and is spatially distinct from the tip of the lamellipodium, we refer to it as a nascent GP actin filament bundle and to the transition from filopodium to nascent GP bundle as conversion. For all conversion events we detected at the temporal resolution of 10–15 s, the front tip of a converted filopodium is initially localized typically toward the rear of the lamellipodium (e.g., Figure 3c, 0 s, and 3h, 0 s) and then as the lamellipodium continues to advance, at the boundary with the lamella (e.g., Figure 3c, 20–100 s, and 3h, 30 s). Conversion from a protrusive filopodium to a nonprotrusive, nascent GP actin bundle is further illustrated (Figure 3d) for the life histories of three individual filopodium (Figure 3d, −200 to 0 s) to GP actin bundle (Figure 3d, 0–200 s) conversion (0 s) events, and for matched pairs of filopodia to GP bundle conversion events for the entire population (Figure 3e).

Once the filopodium has converted, the nascent GP bundle elongates (Figure 3c, 0–100 s, compare guillemets) and also shown for the life histories for three individual GP bundles plotted in Figure 3f (0–200 s). As the GP bundle front tip is net stationary with respect to the substratum (as illustrated in Figure 3, c–e), elongation is apparently rearwards, further into the lamella (Figure 3c, compare guillemets, 0–100 s). Nascent GP bundles elongate an average 1.48 μm/min (Figure 3e) and reach lengths that can be resolved of 3–9 μm (Figure 3f). During the process of elongation the elongating GP bundle meets more mature GP bundles deeper within the lamella (Figure 3c, observable 60–100 s).

To address the possibility that a new GP bundle instead forms in the location previously occupied by a filopodium, rather than directly from it, we performed several tests. First we performed separate time-lapse experiments at 10-fold higher temporal resolution, recording events every 1 s in live cells expressing GFP-actin. We obtained similar data: that 89.5% (51/57) GP bundles are clearly derived from filopodia (Figure 3, g and h; see also Supplemental Movie S5) and 11.5% from subzones within the lamellipodium. This is a similar proportion (Figure 3h) to analysis at 10-s resolution (Figure 3a). Next we measured filopodium length during conversion. In 60% of cases, filopodia do not considerable change length during conversion (defined as less than a 15% change in length; e.g., Figure 3i, compare −10 s and 0 s). For the other 40% of cases, the filopodium shortens slightly during conversion to 70–85% of its original length (e.g., Figure 3c, compare −10 s and 0 s). Because a filopodium destined to form GP bundles, neither shrinks considerably during the process, nor at higher temporal resolution is

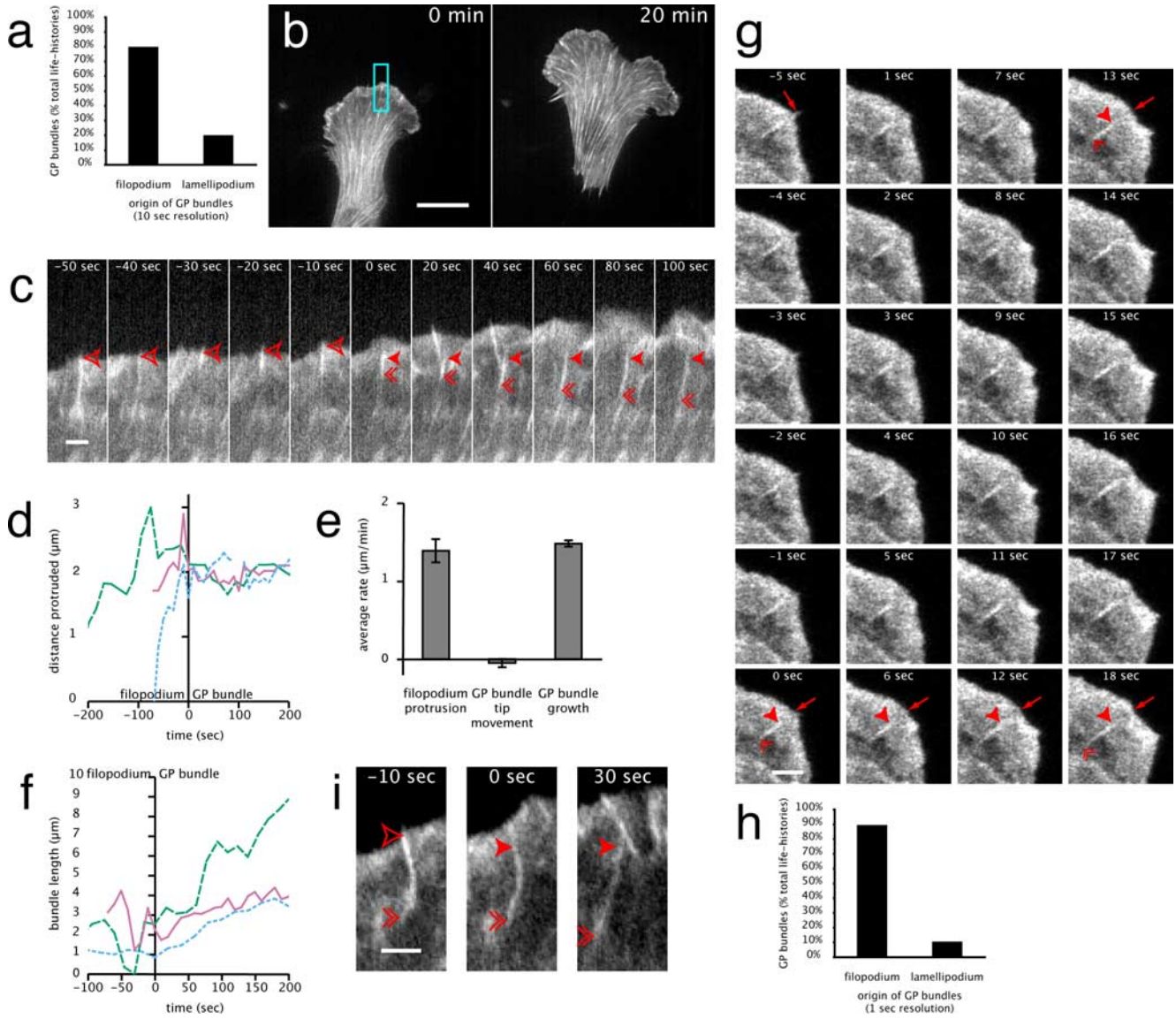

Figure 3. F-actin within filopodia and lamellipodia seed the formation of new GP actin filament bundles within the lamella. The origin of individual GP bundles in live cells expressing GFP-actin was determined from their time-lapse prehistories imaged by spinning disk confocal (a–f and i) or confocal (g and h) microscopy. (a) Quantification of the origin of GP bundles classified as filopodia (fp) or subzones within the lamellipodium (lp) at 10-s temporal resolution (n = 50 events in 10 live cells). (b) An individual cell's migration over 20 min. (c) An enlargement of the boxed region in panel b, showing an individual example of a filopodium (hollow arrowhead, −50 to −10 s) that seeds the formation (0 s) of a nascent GP bundle (solid arrowhead, 0–100 s) and subsequent GP bundle elongation (compare guillemets, 0–100 s). (d) Three individual examples of filopodium-to-GP bundle conversion events (solid magenta line is quantification of the filopodium-to-GP bundle conversion in panel c. (e) Quantification of filopodium protrusion rate (average 1.39 ± 0.15 μm/min) and GP bundle movement at tip (average −0.05 ± 0.005 μm/min; n = 50 individual pairs of filopodium-to-GP bundle conversion events in 10 live cells). (f) Three individual examples of nascent GP bundle elongation (solid magenta line represents the nascent GP bundle imaged in panel c). (g) Higher time resolution (imaged every 1 s) of a filopodium-to-GP bundle conversion event. Arrow either indicates the filopodium (−5 s) or tip of the leading cell edge (0, 6, 12, 13, and 18 s). Conversion of a filopodium to a GP bundle (0 s) is defined as a clear gap between the tip of the leading cell edge (0 s, arrow) and the tip of the filopodium (0 s, arrowhead). Arrowheads indicate the tip of the F-actin bundle and guillemets indicate the rear of the bundle. (h) Quantification of the origin of GP bundles classified as filopodia (fp) or subzones within the lamellipodium (lp) at 1-s temporal resolution (n = 57 events in 11 live cells). (i) Example of a filopodium-to-GP bundle conversion with minimal bundle shortening. Bars, (b) 18 μm, (c, i, and g) 2 μm.

there any evidence of disappearance of the filopodium, this data does not support the possibility that a GP bundle forms in the location previously occupied by a filopodium.

For the minority (20%) of GP bundles that appeared to form directly from subzones within the lamellipodium, the details are similar to that for filopodia, except that the first visualization of the F-actin intensity destined to form a GP bundle appeared directly within the body of the lamellipodium, rather than at its tip as for filopodia. Appearance of these F-actin intensities appeared temporally linked either with a localized protrusive burst (8% of cases) or from a region of lamellipodium that was protruding and then underwent a small retraction (12%). It has been shown that the first stage in filopodium formation is a localized elongation

of actin filaments within the lamellipodium (Svitkina *et al.*, 2003), and we speculate that some of the F-actin intensities that we observed to appear directly within the lamellipodium may have been early-stage filopodia, which instead of producing filopodia instead converted to GP bundles.

Overall, the observed dynamic and structural link between actin filaments in the leading cell edge and GP bundles at the front of the lamella agree very well. However, the EM data (Figure 1g) could infer a roughly equal proportion of GP bundles derived from filopodia and subzones within the lamelli-

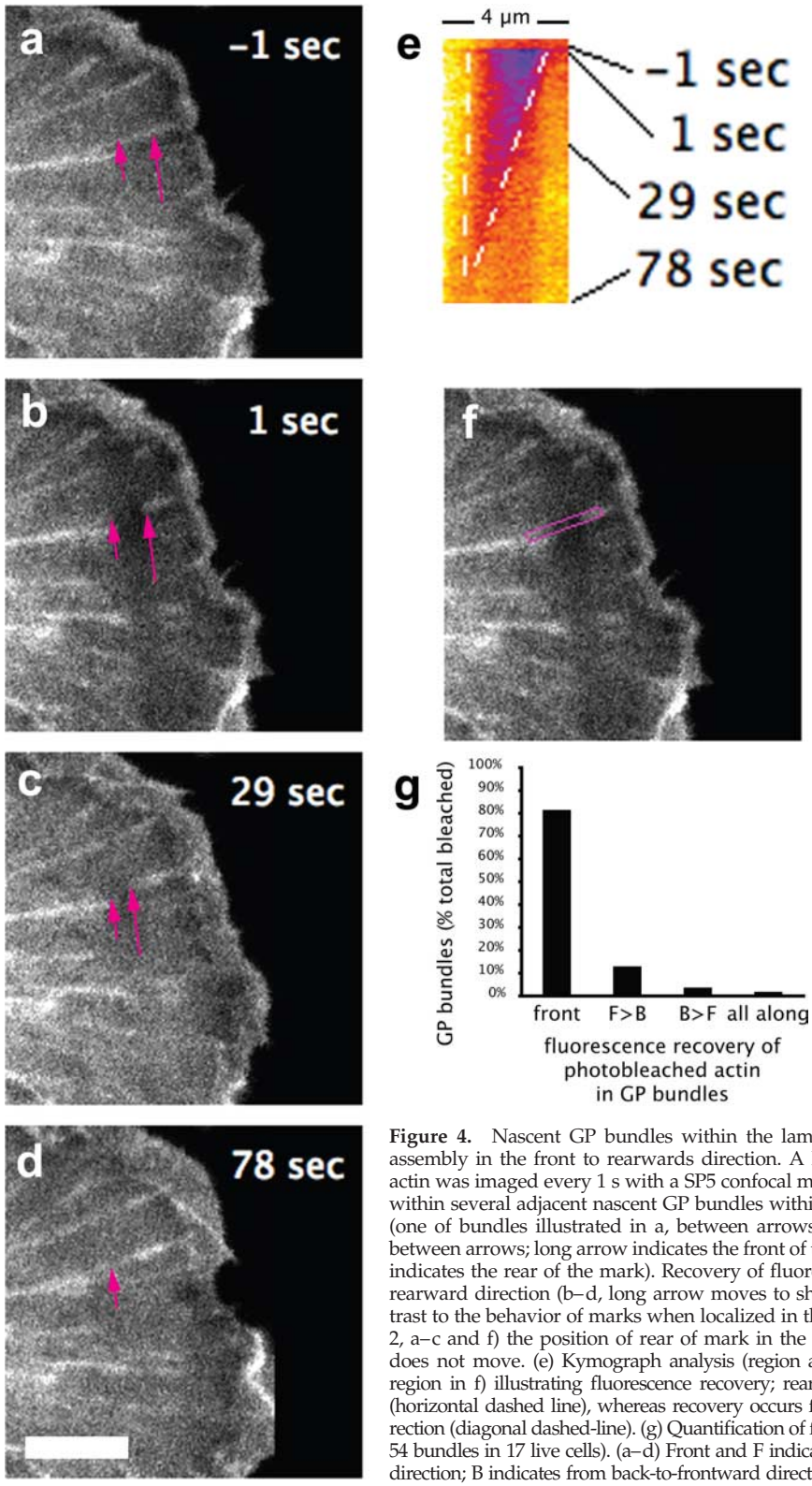

Figure 4. Nascent GP bundles within the lamella elongate by subunit assembly in the front to rearwards direction. A live cell expressing GFP-actin was imaged every 1 s with a SP5 confocal microscope, and a subzone within several adjacent nascent GP bundles within the front of the lamella (one of bundles illustrated in a, between arrows) was photobleached (b, between arrows; long arrow indicates the front of the mark and short arrow indicates the rear of the mark). Recovery of fluorescence is in the front-to-rearward direction (b–d, long arrow moves to short arrow). Note, in contrast to the behavior of marks when localized in the lamellipodium (Figure 2, a–c and f) the position of rear of mark in the GP bundle (short arrow) does not move. (e) Kymograph analysis (region analyzed shown in boxed region in f) illustrating fluorescence recovery; rear of mark does not move (horizontal dashed line), whereas recovery occurs from front-to-rearward direction (diagonal dashed-line). (g) Quantification of fluorescence recovery (n = 54 bundles in 17 live cells). (a–d) Front and F indicate from front-to-rearward direction; B indicates from back-to-frontward direction. Bar, (d) 5 μm.

podium. We presume some of the filaments scored as lamellipodial in the EM work could be late-stage filopodial-conversion events as appearance in fixed cells would be similar in these two situations. In addition detection of events derived from the lamellipodium in live cells expressing GFP-actin may be at the limits of detection of our microscopy system.

Elongation of Newly Formed GP Bundles Occurs Primarily by Addition of Actin Subunits from the Front to Backward Direction

To test where subunits add to a nascent GP bundle during GP bundle elongation, we assessed photobleached marks made directly within newly formed GP bundles within the lamella in live migrating cells. As expected from previous photoactivation of fluorescence studies (Cramer *et al.*, 1997), and from the data in Figure 2 photobleached marks made directly within GP bundles within the lamella remained stationary with respect to the substratum as the cell advanced (Figure 4, a–d, and vertical line in the kymograph in e). In addition to this expected behavior, fluorescence recovered from the front of the bleached zone (Figure 4, a–d, and diagonal line in the kymograph in e) within the GP bundle (see also Supplemental Movie S6). Recovery from the front is the expected outcome if new GFP-actin subunit addition is primarily in the front-to-backward direction. Quantification of the population (Figure 4g) shows that in bleached marks made within the lamella on GP bundles, fluorescence recovery was either only from the front (44/51) as far as we could detect and measure or apparently mainly from the front and less from the back (7/51). Thus in 51/54 (94.4%) cases fluorescence recovery is entirely or mainly from the front. A small minority of 2/54 (3.7%) bleached zones apparently recovered mainly from the back and less from the front, and a further tiny minority (1/54) bleached marks appeared to recover all along the zone (Figure 4g).

Myosin II Is Localized within the Leading Cell Edge Mostly at the Rear

Myosin II is present in GP bundles throughout their length (Cramer *et al.*, 1997). Myosin II must therefore become incorporated into GP bundles at some point during their formation. The conventional view has been that myosin II is excluded from the leading cell edge of motile cells. However myosin II is localized to more mature protrusions (DeBiasio *et al.*, 1988), and in more recent work was detectable within (Svitkina *et al.*, 1997; Schaub *et al.*, 2007) or close to (Verkhovsky *et al.*, 1995) the lamellipodium in motile cells and between the peripheral and central domain of neuronal growth cones (Medeiros *et al.*, 2006). To begin to ask the role of myosin II in GP bundle formation, we looked in detail at the distribution of myosin II in migrating fibroblasts in fixed cells (Figure 5). Superficial observation of myosin II does not readily show leading cell edge localization when compared with localization of myosin II in GP actin bundles generally in cells (Figure 5b). However, more detailed analysis shows a clear, smaller proportion of myosin II localized within the leading cell edge (Figure 5e, arrowheads). We detected myosin II puncta within the leading cell edge in 89% of fixed cells (Figure 5g). In these cells, 87% of myosin II puncta is localized at the rear of the leading cell edge at the boundary with the lamella (Figure 5, h and e, upper arrowheads), and the remaining 13% minority of myosin II puncta localized deeper in the leading cell edge (Figure 5, h and e, lower arrowhead). Sixty-nine percent of myosin II puncta within the

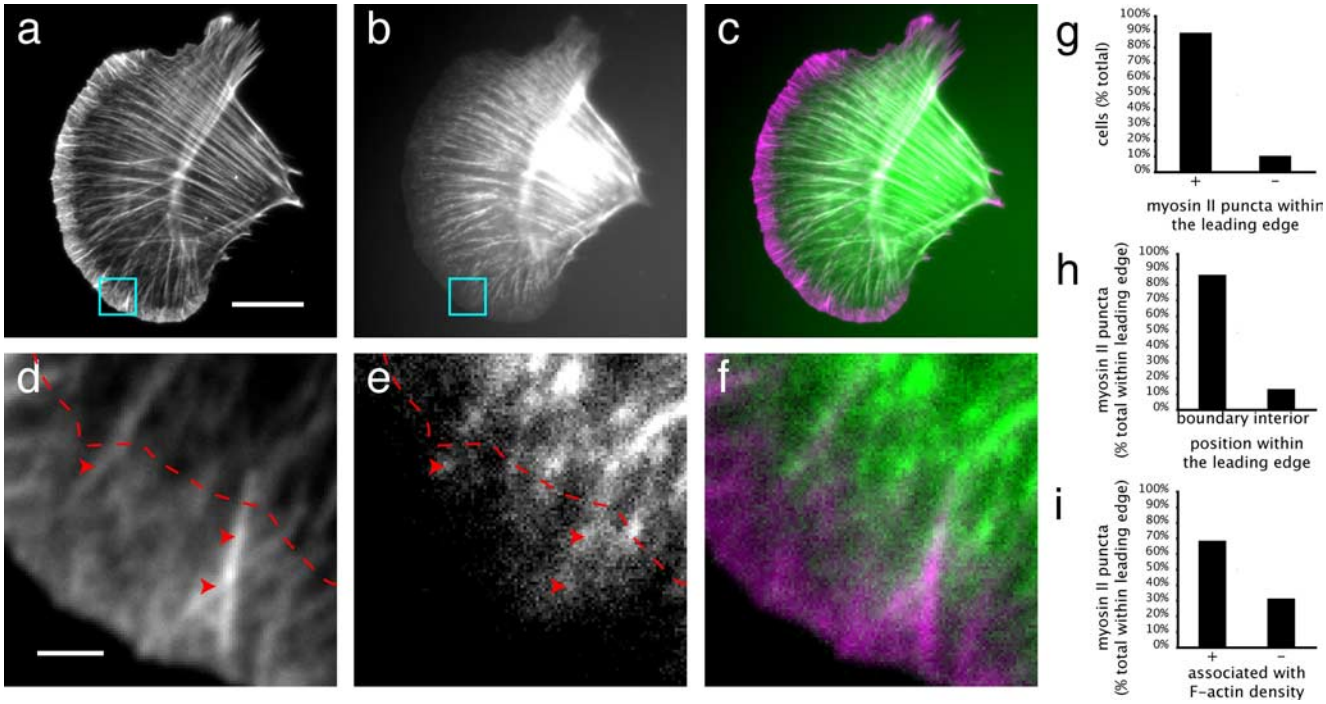

Figure 5. Myosin II puncta localize to the leading cell edge. Cell expressing GFP-myosin II light chain (b and e) fixed and costained for F-actin with Alexa 594-phalloidin (a and d). (d and e) Enlarged view of the box in a and b, respectively. (c and f) Overlay images. Note, myosin II puncta (e, arrowheads) are localized within the leading cell edge (below dashed line) and at the rear of the leading cell edge at the boundary with the lamella (dashed line). (g) Quantification of cells with myosin II puncta detected in the leading cell edge (le). (h) Quantification of position of myosin II puncta detected in the leading cell edge (le). (i) Quantification of myosin II puncta associated with F-actin intensity in the leading cell edge (le) (for panels g–i, n = 127 puncta in 19 cells). Bar, (a) 10 μm, (d) 1 μm.

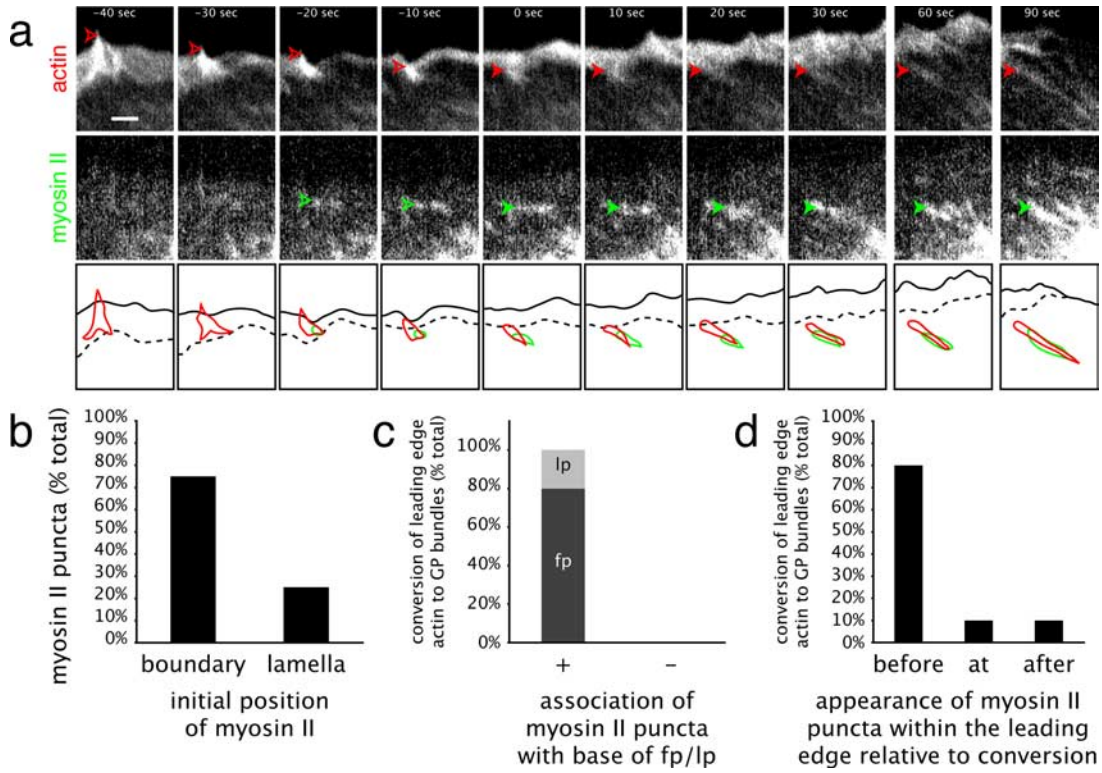

Figure 6. Myosin II localizes to filopodia destined to form GP actin filament bundles. Live cell expressing both RFP-actin (a, top panels) and GFP-myosin II light chain (a, middle panels) was imaged by dual-color time-lapse spinning disk confocal microscopy (both F-actin in red and myosin II in green are traced in the bottom panels). Conversion of a filopodium (hollow arrowheads) to a GP bundle (solid arrowheads) is illustrated. Time (sec) is relative to conversion (0 s). (b) Quantification of initial spatial location of detected myosin II puncta destined to associate with a nascent GP bundle (n = 20 events in four live cells). Boundary indicates boundary of the leading cell edge and lamella. (c) Quantification of spatial position of myosin II associated with F-actin destined to convert to a GP bundle. (d) Quantification of relative temporal association of myosin II with a filopodium destined to form a GP bundle (for c and d, n = 10 conversion events in two live cells). Bar, (a) 2 μm.

leading cell edge, is clearly associated with F-actin intensities in this region (Figure 5, i and 5, d and e; compare arrowheads). We obtained similar results using an antibody to endogenous myosin II heavy chain (data not shown) and when expressing myosin II light-chain–tagged with GFP in cells (Figure 5).

Dynamics of Myosin II during Formation of Nascent GP Bundles in Live Cells

To continue investigation of the role of myosin II in nascent GP bundle formation we assessed dynamics in live cells expressing both mRFP-actin and EGFP-myosin II essential light chain (see *Materials and Methods*). Because of the required use of two viral infections in the same cell, good cell health was offset with lower levels of fluorescence intensity for each probe expressed than when only one probe is expressed (see *Materials and Methods*). With this limitation we detected three myosin II dynamic behaviors in the context of nascent GP bundle formation (Figure 6). First, myosin II puncta in live cells, consistent with the analysis in fixed cells is mostly initially localized to the rear of the leading cell edge (Figure 6, a and b) at the base of filopodia (Figure 6a, −20, −10 s, 0 s, compare red and green outline on the trace, and Figure 6c). Second, myosin II within the leading cell edge associates with lamellipodium or filopodium F-actin that is destined to form GP bundles (Figure 6a, compare time intervals, open and solid arrowheads, which are quantified in Figure 6c) an average 28 ± 11 s (ranging 0–1 min 15 s in 11 events) before the conversion of that filopodium or lamellipodium F-actin (Figure 6a, compare −20 s and 0 s) to a GP bundle (see also quantification in Figure 6d). Third, myosin II puncta associated with nascent GP bundles appear stationary with respect to the substratum (Figure 6a, 0–90 s, compare solid arrowheads) and continues to associate with F-actin during subsequent bundle elongation (Figure 6a, 30–90 s, compare solid arrowheads).

Myosin II Is Required for the Relocalization of Leading Edge F-Actin Seeds to the Lamella

The prior association of myosin II with filopodia that are destined to form GP actin bundles (Figure 6) suggests myosin II may be required for the relocalization of leading edge F-actin seeds to the lamella. We tested this by treating live fibroblasts expressing mRFP-actin with 100 μM (±) blebbistatin, a specific inhibitor of myosin II ATPase activity (Straight *et al.*, 2003). Within 10 min 100 μM blebbistatin treatment appearance of new GP bundles within the lamella fell 10-fold (Figure 7b, compare top and bottom panels, and Figure 7c). Inhibition of appearance of new GP bundles cannot be explained by a general block of filopodia or lamellipodium protrusion as these are not inhibited (Figure 7a, compare 0 and 10 min) over the 10-min time scale, where appearance of new GP bundles is blocked. In addition more mature GP actin bundles deeper in the cell, existing before addition of blebbistatin, remained during 10-min blebbistatin treatment (Figure 7a, 10 min, compare presence of bundles located deeper in the cell), indicating that the treatment

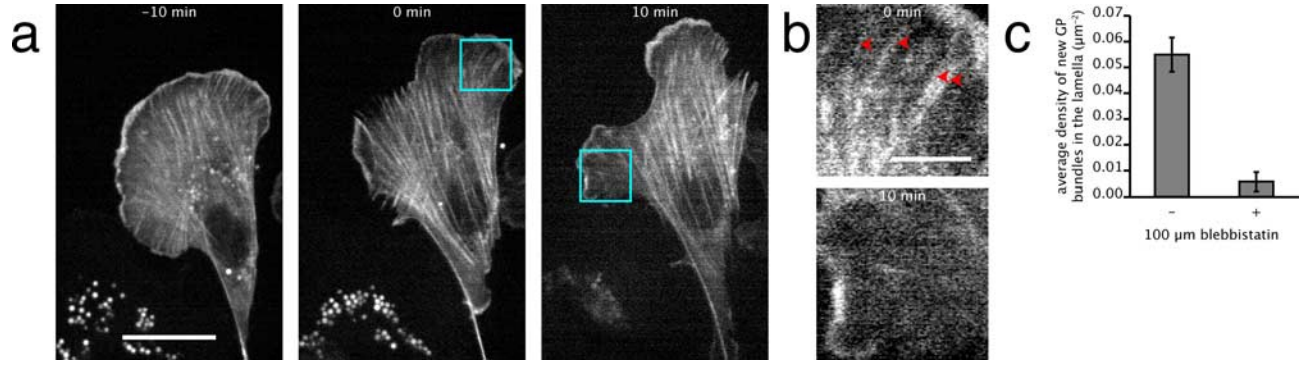

Figure 7. Myosin II ATPase activity is required for appearance of new GP bundles in the lamella. Live cell infected and expressing RFP-actin only and treated with 100 μM (±)-blebbistatin to block myosin II activity; time in panel a indicates minutes relative to addition of the inhibitor. Boxes in panel a indicate the area of greatest protrusion over the preceding 10 min. (b) Enlargements of the boxed areas in panel a; arrowheads indicate GP bundles. Note the absence of new GP bundles in the lamella during 10-min blebbistatin treatment (bottom panel). (c) Quantification of the entire front of the lamella of the density of GP actin bundles before (an average 0.055 ± 0.007 per μm^2) and after (an average 0.006 ± 0.004 per μm^2) addition of 100 μM (±)-blebbistatin for 10 min in the same live cell (n = eight live cells). Bars, (a) 20 μm, (b) 5 μm.

had not generally disrupted GP bundles. Finally, myosin II localization within the lamellipodium appears unaffected in cells treated for 10 min with blebbistatin (data not shown), thus the possibility of mislocalized myosin II cannot explain the block in appearance of new GP bundles within the lamella. With longer treatment (up to 45 min) of cells with blebbistatin, GP actin filament bundles are not detected throughout the cell (data not shown).

DISCUSSION

Taking these data together, retrograde flow of actin filaments within the leading cell edge delivers F-actin to the boundary with the lamella where it seeds formation of GP actomyosin II filament bundles that are stationary with respect to the substratum and that relocalization of the F-actin seed within the lamella requires myosin II ATPase activity (Figure 8).

Structural Link Between Actin Filaments within the Leading Cell Edge and GP Bundles within the Lamella in Migrating Fibroblasts

The structural relationship between actin filaments within the leading cell edge and deeper in the cell has not been widely explored in migrating cell types. One exception is in migrating keratocytes (Svitkina *et al.*, 1997) and fish fibroblasts (Nemethova *et al.*, 2008), where these two zones are structurally linked, though the orientation of bundles in these two cell types are distinct to GP bundles in chick fibroblasts. The orientation of GP bundles in fibroblasts is more similar to several neuronal growth cones where filopodial bundles extend deep into the growth cone (Lewis and Bridgman, 1992; Mallavarapu and Mitchison, 1999; Medeiros *et al.*, 2006) and may be analogous to the link between filopodia and GP bundles

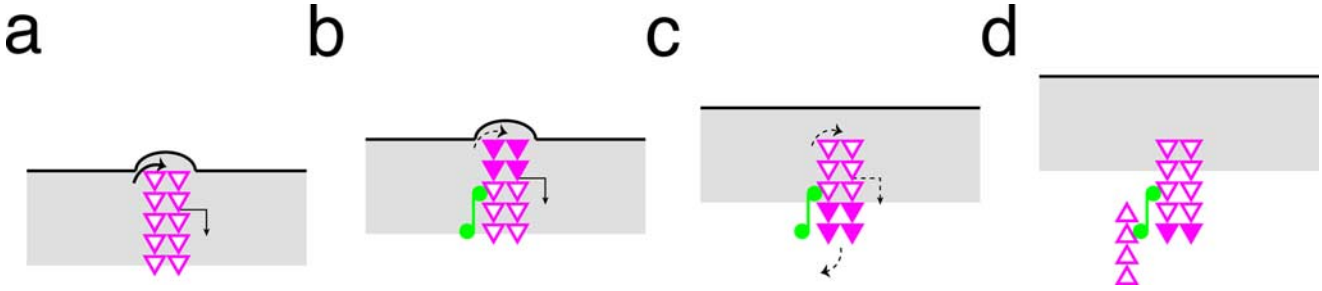

Figure 8. Retrograde flow delivers F-actin to the lamella to seed the formation of GP bundles. A simplified schematic based on data on F-actin and myosin II dynamics and actin filament polarity from our current and previous work in migrating fibroblasts and other cited information (see text for details). Observed behavior of marked F-actin (closed magenta chevrons) in the lamellipodium (gray stripe) and lamella (white region) is represented. (a, protrusion) local F-actin in a filopodium or subzone within the lamellipodium (magenta chevrons) undergoing retrograde flow (bent arrow) assembles at its tip (curly-on arrow) at the same rate as bulk F-actin within the leading cell edge (gray stripe). Not shown, for simplicity, is F-actin disassembly, which also occurs within the F-actin network. (b, association of myosin II) A myosin II punctum (green dumb-bell) associates with the base of the local F-actin region (magenta chevrons) destined to form a GP bundle. (b and c, conversion) Local F-actin continues to flow retrograde (bent arrow) as local assembly rate slows down (dashed curly-on arrow), whereas net cell protrusion (black line) is driven at the prior assembly rate. This results in separation (gap in c) of the tip of the local F-actin region from the tip of the leading cell edge. (c and d, F-actin seed) This process delivers an F-actin seed (magenta chevrons) to the boundary (interface of white and gray regions) of the leading cell edge (gray stripe) and the lamella (white region). Detectable retrograde F-actin flow slows down/stops (dashed bent arrow) in the seed through activation of cell–substratum adhesion formation. (d, GP bundle elongation) Associated myosin II (green dumb-bells) promotes recruitment of oppositely opposed actin filaments, as required for graded polarity in this region. Actin subunits during elongation (compare c and d, open chevrons) mainly assemble at filament barbed-ends in the front-to-rear direction. Our data predicts either balanced local actin disassembly in the original F-actin seed at conversion to a GP bundle (c, dashed curly-off arrow) and/or GP bundle elongation is driven primarily by addition of subunits recruited to associated myosin II (c and d, compare open chevrons).

described here, although actin filament polarity is not known for these long filopodia as a function of proximal-distal bundle position.

Dynamic Link between Actin Filaments within the Leading Cell Edge and GP Bundles in the Lamella in Migrating Fibroblasts

Our data here together with our previous work in migrating fibroblasts (Cramer *et al.*, 1997, 1999b; Dawe *et al.*, 2003) implies that for fibroblast cell migration a proportion of actin filaments within the leading cell edge must be removed from the recyclable pool in this location to seed formation of GP bundles at the boundary with the lamella. How might these steps occur?

For the delivery of the F-actin seed to the boundary with the lamella, the observed structural link at this boundary between actin filaments in the leading cell edge and GP bundles in the lamella (Figure 1), and dynamic evidence linking retrograde flow of F-actin within the leading cell edge to GP bundles within the lamella (Figure 2) infers strongly that delivery of the seed is at least in part driven by retrograde F-actin flow (Figure 8, b and c). It is also expected that differences in local actin assembly rate at the tip of the F-actin seed and bulk leading cell edge also contribute, as filopodia stop protruding during conversion to GP bundles (Figures 3 and 8, b and c). In some cells, retrograde F-actin flow has been explained as a mechanism to slow leading edge net protrusion rate (Lin and Forscher, 1995; Mallavarapu and Mitchison, 1999; Giannone *et al.*, 2004). A contribution of retrograde F-actin flow for the delivery of F-actin seeds to construct new actin assembles elsewhere in the cell, as described here, is arguably the first explicitly identified direct reason for the existence of this flow in cells.

Once the F-actin seed is delivered to the lamella, it then apparently stops flowing (Figures 2, 4, and 8, c and d), consistent with known stationary behavior of F-actin within GP bundles in this location in these cells (Cramer *et al.*, 1997). In some motile cell types an apparent collision of separate populations of rearward- and forward-flowing F-actin explains a small zone a few micrometers deep of stationary F-actin with respect to the substratum (Salmon *et al.*, 2002; Vallotton *et al.*, 2004; Schaub *et al.*, 2007). However, this is an unlikely explanation for the cessation of movement of F-actin seeds in migrating fibroblasts because there is no evidence for a significant population of forward-flowing F-actin in the lamella region of migrating chick fibroblasts (this work and Cramer *et al.*, 1997). There is a population of actin filaments that moves forward in these cells, but this is well separated from the lamella zone in these cells (Cramer *et al.*, 1997). However we do not rule out the possibility that a collision band may be present, but as yet undetected in fibroblasts.

In the absence of any existing evidence for a collision of opposite flows of F-actin in these cells, we favor the idea that cessation of rearward-flowing F-actin seeds in these situations is driven by anchoring the nascent GP bundle to the substratum within the lamella, and as best fits our data (Figure 2), this occurs at the boundary of the leading cell edge and lamella. GP bundles are associated with the adhesion protein talin at the ventral cell surface (Cramer *et al.*, 1997), and talin is also associated with filopodia in these cells (our unpublished observations). Also, strikingly, activators of cell–substratum adhesion are carried on rearward-flowing F-actin within the lamellipodium (Giannone *et al.*, 2004); we envisage that these activators could anchor the same flowing population of F-actin to the substratum in the formation of a GP bundle.

Clearly, not all F-actin undergoing retrograde F-actin flow within the leading cell edge is removed from the recyclable pool to seed new GP bundles at the boundary with the lamella in migrating fibroblasts. A proportion must also be depolymerized by ADF/cofilin to produce actin monomer fuel to power leading cell edge protrusion in these cells (Cramer, 1999b; Dawe *et al.*, 2003; Bernstein and Bamburg, 2004). How these two pathways are spatially and temporally separated within the leading cell edge is an interesting avenue for future exploration.

Function of Myosin II in Formation of GP Bundles within the Lamella

In the context of F-actin assemblies in cells, myosin II has roles in both promoting assembly of the actin structure and in disassembling them (Burgess, 2005; Medeiros *et al.*, 2006; Haviv *et al.*, 2008). Combined, the simplest explanation of our data (Figures 5–7) is that myosin II activity within the leading cell edge is specifically required for relocating the F-actin seed from this location to the lamella in the formation of new GP bundles. This pin-points a spatial role for myosin II, in that it determines where a bundle is to form in cells, a new role for myosin II in the construction of bundles. What is the precise nature of this spatial role? Two functions are plausible. One function is that myosin II contributes to the force driving retrograde flow (Lin *et al.*, 1996; Henson *et al.*, 1999; Vallotton *et al.*, 2004; Medeiros *et al.*, 2006; Zhou and Wang, 2008) of the F-actin seed (Figure 8, b and c). Although the precise location in cells of myosin II–based- F-actin retrograde flow has been argued, recently it has been clearly shown to play a major role in retrograde F-actin flow within the lamellipodium (Medeiros *et al.*, 2006). A second nonexclusive role, to satisfy known stationary behavior of the F-actin seed once it reaches the lamella (this work and Cramer *et al.*, 1997; Figure 8, c and d) is that myosin II ATPase activity couples the flowing F-actin seed with formation of new adhesions within the lamella. This idea is supported by the observation that myosin II activity is needed for adhesion formation (Chrzanowska-Wodnicka and Burridge, 1996; Giannone *et al.*, 2007).

Both these precise roles for myosin II in migrating fibroblasts require a prior association of myosin II with F-actin destined to seed new GP bundles and that myosin II itself is stationary with respect to the substratum when associated with newly formed GP bundles in these cells, both as experimentally observed in these cells (Figure 6). In other motile cells types, myosin II is also associated with F-actin within filopodia (Medeiros *et al.*, 2006) and the lamellipodium (DeBiasio *et al.*, 1988; Svitkina *et al.*, 1997; Verkhovsky *et al.*, 1999; Giannone *et al.*, 2007; Schaub *et al.*, 2007) and is stationary with respect to the substratum in these locations in migrating cells (Svitkina *et al.*, 1997; Verkhovsky *et al.*, 1999). Myosin II has also been observed to move retrograde in cells (McKenna *et al.*, 1989; Giuliano and Taylor, 1990; Conrad *et al.*, 1993; Svitkina *et al.*, 1997; Verkhovsky *et al.*, 1999). However, the stationary- or retrograde-dynamic behavior of myosin II is a function of cell migration and cessation of migration respectively (Svitkina *et al.*, 1997; Verkhovsky *et al.*, 1999).

Generation of Graded Filament Polarity Organization and GP Bundle Elongation

Subsequent steps in GP bundle formation include generation of known (Cramer *et al.*, 1997) graded filament polarity and observed (Figures 3, 4, and 6) bundle elongation.

For filament polarity, at the front of the lamella, more than 80% of actin filaments in a graded polarity actin filament bundle in this location are oriented with filament plus ends facing the direction of migration (Cramer *et al.*, 1997). As filopodia do not change spatial orientation during formation of GP bundles, this proportion is mainly explained then by the filament polarity within the original filopodium or subzone within the lamellipodium (Figure 8). The remaining ~20% of filaments required with filament minus ends facing forward in this location could be generated during elongation of the nascent GP actin bundle (Figure 8d). Because myosin II is localized to filopodia destined to form GP actin bundles and continues to further associate with F-actin during GP bundle elongation (Figure 6), it is temporally and spatially well placed to promote oppositely opposed filaments within the bundle. One possibility is via myosin II–mediated recruitment of actin subunits (Neujahr *et al.*, 1997; Bi *et al.*, 1998; Olazabal *et al.*, 2002; Urven *et al.*, 2006), but see (Zhou and Wang, 2008) and myosin II–mediated polarity sorting of assembled actin (Nakazawa and Sekimoto, 1996; Figure 8d). This scenario is also attractive as it explains observed addition of actin subunits in the front-to-rearwards direction (Figure 4) without apparent movement of the tip of the GP bundle (Figures 3 and 6) or apparent rearward F-actin flow within the GP bundle in this location (Figure 4; Cramer *et al.*, 1997; Figure 8d). Thus in this way, the original F-actin seed to make a GP bundle at the front of the cell is derived from actin filaments within the leading cell edge (Figure 8, b and c), whereas GP bundle elongation is mainly driven by assembly of subunits within the lamella (Figure 8, c and d).

We did not address in this study, formation of GP actin filament bundles located deeper within the cell, an extensive body of work in its own right.

F-Actin Seeds Derived from the Leading Cell Edge, a New Pathway to Make Actin Filament Bundles in the Cell Body in Migrating Cells

Our data provides evidence for the principles of an older idea (Heath, 1983; Heath and Holifield, 1993) originally based on indirect data, that arcs, a type of transverse actin filament bundle observed in some cell types, originate from actin filaments at the rear of the lamellipodium, recently supported by RNAi experiments (Supplementary Figure S2, Machesky and Insall, 1998; Hotulainen and Lappalainen, 2006). Similarly, another type of arc, dorsal actin fibers, which are oriented in the direction of migration also appear to originate at the rear of the lamellipodium (Hotulainen and Lappalainen, 2006). In migrating keratocytes formation of transverse actomyosin II filament bundles located at the front of the cell body in these cells involves actin filaments originating within the lamellipodium (Svitkina *et al.*, 1997; Verkhovsky *et al.*, 1999), flowing retrograde to the site of bundle assembly (Vallotton *et al.*, 2005; Schaub *et al.*, 2007) or by separate lateral flow of actin filaments (Small *et al.*, 1998; Small and Resch, 2005).

Filopodia have also been observed to form actin bundles in the lamella of fish fibroblasts and B16 melanoma cells (Nemethova *et al.*, 2008). It seems this mostly occurs by lateral folding of individual filopodia into the lamella. This is likely a distinct filopodia-based mechanism to the one uncovered here in primary migrating fibroblasts where folding of filopodia does not occur during GP bundle formation and, unlike delivery of filopodium F-actin to seed GP bundles, myosin II is not required for filopodium folding (Nemethova *et al.*, 2008). Further comparison is not possible as in contrast to migrating fibroblasts, there is no information on F-actin dynamics or actin filament polarity in the folding-filopodium study.

Interestingly, outside of migrating cell types, actin filaments within microvilli, a cell surface feature seed the formation of radial actin filament bundles within the cell body of nurse cells in *Drosophila* (Guild *et al.*, 1997).

Using F-actin seeds from within lamellipodia, filopodia, and other cell surface features may turn out an important pathway for the formation in other spatial locations in cells of a variety of actin filament structures.

Actin filaments within the leading cell edge delivered by retrograde flow to seed new actomyosin II filament bundles in the cell body provides an important mechanism for structurally and dynamically linking cell protrusion and cell tension needed for overall coordination during fibroblast migration.

ACKNOWLEDGMENTS

We thank Professor Jim Bamburg (Colorado State University) for supplying the GFP-actin and RFP-actin adenoviral constructs, Dr. Lindsay Hewlett for performing the whole mount microscopy, and Ms. Tayamika Mseka and Dr. Buzz Baum for helpful comments on the manuscript. L.P.C. is a Royal Society University Research Fellow, and T.W.A. was supported by an MRC studentship. The work was supported by grants from the Cancer Research UK and Wellcome Trust (L.P.C.).

REFERENCES

Badley, R. A., Couchman, J. R., and Rees, D. A. (1980). Comparison of the cell cytoskeleton in migratory and stationary chick fibroblasts. J. Muscle Res. Cell Motil. *1*, 5–14.

Bernstein, B. W., and Bamburg, J. R. (2004). A proposed mechanism for cell polarization with no external cues. Cell Motil. Cytoskelet. *58*, 96–103.

Bi, E., Maddox, P., Lew, D. J., Salmon, E. D., McMillan, J. N., Yeh, E., and Pringle, J. R. (1998). Involvement of an actomyosin contractile ring in *Saccharomyces cerevisiae* cytokinesis. J. Cell Biol. *142*, 1301–1312.

Burgess, D. R. (2005). Cytokinesis: new roles for myosin. Curr. Biol. *15*, R310–R311.

Carlier, M. F., and Pantaloni, D. (2007). Control of actin assembly dynamics in cell motility. J. Biol. Chem. *282*, 23005–23009.

Chrzanowska-Wodnicka, M., and Burridge, K. (1996). Rho-stimulated contractility drives the formation of stress fibers and focal adhesions. J. Cell Biol. *133*, 1403–1415.

Conrad, P. A., Giuliano, K. A., Fisher, G., Collins, K., Matsudaira, P. T., and Taylor, D. L. (1993). Relative distribution of actin, myosin I, and myosin II during the wound healing response of fibroblasts. J. Cell Biol. *120*, 1381–1391.

Couchman, J. R., and Rees, D. A. (1979). The behaviour of fibroblasts migrating from chick heart explants: changes in adhesion, locomotion and growth, and in the distribution of actomyosin and fibronectin. J. Cell Sci. *39*, 149–165.

Cramer, L. P. (1997). Molecular mechanism of actin-dependent retrograde flow in lamellipodia of motile cells. Front. Biosci. *2*, d260–d270.

Cramer, L. P. (1999a). Organization and polarity of actin filament networks in cells: implications for the mechanism of myosin-based cell motility. Biochem. Soc. Symp. *65*, 173–205.

Cramer, L. P. (1999b). Role of actin-filament disassembly in lamellipodium protrusion in motile cells revealed using the drug jasplakinolide. Curr. Biol. *9*, 1095–1105.

Cramer, L. P., Briggs, L. J., and Dawe, H. R. (2002). Use of fluorescently labelled deoxyribonuclease I to spatially measure G-actin levels in migrating and non-migrating cells. Cell Motil. Cytoskelet. *51*, 27–38.

Cramer, L. P., Siebert, M., and Mitchison, T. J. (1997). Identification of novel graded polarity actin filament bundles in locomoting heart fibroblasts: implications for the generation of motile force. J. Cell Biol. *136*, 1287–1305.

Dawe, H. R., Minamide, L. S., Bamburg, J. R., and Cramer, L. P. (2003). ADF/cofilin controls cell polarity during fibroblast migration. Curr. Biol. *13*, 252–257.

DeBiasio, R. L., Wang, L. L., Fisher, G. W., and Taylor, D. L. (1988). The dynamic distribution of fluorescent analogues of actin and myosin in protrusions at the leading edge of migrating Swiss 3T3 fibroblasts. J. Cell Biol. *107*, 2631–2645.

Faix, J., and Rottner, K. (2006). The making of filopodia. Curr. Opin. Cell Biol. *18*, 18–25.

Forscher, P., and Smith, S. J. (1990). Cytoplasmic actin filaments move particles on the surface of a neuronal growth cone. In: Optical Microscopy for Biology, ed. K. Jacobson and B. Hermann, New York: Wiley-Liss, 459–471.

Giannone, G., Dubin-Thaler, B. J., D'bereiner, H. G., Kieffer, N., Bresnick, A. R., and Sheetz, M. P. (2004). Periodic lamellipodial contractions correlate with rearward actin waves. Cell *116*, 431–443.

Giannone, G. *et al.* (2007). Lamellipodial actin mechanically links myosin activity with adhesion-site formation. Cell *128*, 561–575.

Giuliano, K. A., and Taylor, D. L. (1990). Formation, transport, contraction, and disassembly of stress fibers in fibroblasts. Cell Motil. Cytoskelet. *16*, 14–21.

Guild, G. M., Connelly, P. S., Shaw, M. K., and Tilney, L. G. (1997). Actin filament cables in *Drosophila* nurse cells are composed of modules that slide passively past one another during dumping. J. Cell Biol. *138*, 783–797.

Gupton, S. L., and Gertler, F. B. (2007). Filopodia: the fingers that do the walking. Sci. STKE *2007*, re5.

Haviv, L., Gillo, D., Backouche, F., and Bernheim-Groswasser, A. (2008). A cytoskeletal demolition worker: myosin II acts as an actin depolymerization agent. J. Mol. Biol. *375*, 325–330.

Heath, J. P. (1983). Behaviour and structure of the leading lamella in moving fibroblasts. I. Occurrence and centripetal movement of arc-shaped microfilament bundles beneath the dorsal cell surface. J. Cell Sci. *60*, 331–354.

Heath, J. P., and Holifield, B. F. (1991). Cell locomotion: new research tests old ideas on membrane and cytoskeletal flow. Cell Motil. Cytoskelet. *18*, 245–257.

Heath, J. P., and Holifield, B. F. (1993). On the mechanisms of cortical actin flow and its role in cytoskeletal organisation of fibroblasts. Symp. Soc. Exp. Biol. *47*, 35–56.

Henson, J. H., Svitkina, T. M., Burns, A. R., Hughes, H. E., MacPartland, K. J., Nazarian, R., and Borisy, G. G. (1999). Two components of actin-based retrograde flow in sea urchin coelomocytes. Mol. Biol. Cell *10*, 4075–4090.

Hotulainen, P., and Lappalainen, P. (2006). Stress fibers are generated by two distinct actin assembly mechanisms in motile cells. J. Cell Biol. *173*, 383–394.

Lauffenburger, D. A., and Horwitz, A. F. (1996). Cell migration: a physically integrated molecular process. Cell *84*, 359–369.

Lewis, A. K., and Bridgman, P. C. (1992). Nerve growth cone lamellipodia contain two populations of actin filaments that differ in organization and polarity. J. Cell Biol. *119*, 1219–1243.

Lin, C. H., Espreafico, E. M., Mooseker, M. S., and Forscher, P. (1996). Myosin drives retrograde F-actin flow in neuronal growth cones. Neuron *16*, 769–782.

Lin, C. H., and Forscher, P. (1995). Growth cone advance is inversely proportional to retrograde F-actin flow. Neuron *14*, 763–771.

Machesky, L. M., and Insall, R. H. (1998). Scar1 and the related Wiskott-Aldrich syndrome protein, WASP, regulate the actin cytoskeleton through the Arp2/3 complex. Curr. Biol. *8*, 1347–1356.

Mallavarapu, A., and Mitchison, T. (1999). Regulated actin cytoskeleton assembly at filopodium tips controls their extension and retraction. J. Cell Biol. *146*, 1097–1106.

Mattila, P. K., and Lappalainen, P. (2008). Filopodia: molecular architecture and cellular functions. Nat. Rev. Mol. Cell Biol. *9*, 446–454.

McKenna, N. M., Wang, Y. L., and Konkel, M. E. (1989). Formation and movement of myosin-containing structures in living fibroblasts. J. Cell Biol. *109*, 1163–1172.

Medeiros, N. A., Burnette, D. T., and Forscher, P. (2006). Myosin II functions in actin-bundle turnover in neuronal growth cones. Nat. Cell Biol. *8*, 215–226.

Minamide, L. S., Shaw, A. E., Sarmiere, P. D., Wiggan, O., Maloney, M. T., Bernstein, B. W., Sneider, J. M., Gonzalez, J. A., and Bamburg, J. R. (2003). Production and use of replication-deficient adenovirus for transgene expression in neurons. Methods Cell Biol. *71*, 387–416.

Mitchison, T. J., and Cramer, L. P. (1996). Actin-based cell motility and cell locomotion. Cell *84*, 371–379.

Nakazawa, H., and Sekimoto, K. (1996). Polarity sorting in a bundle of actin filaments by two-headed myosins. J. Phys. Soc. Jpn. *65*, 2404–2407.

Nemethova, M., Auinger, S., and Small, J. V. (2008). Building the actin cytoskeleton: filopodia contribute to the construction of contractile bundles in the lamella. J. Cell Biol. *180*, 1233–1244.

Neujahr, R., Heizer, C., and Gerisch, G. (1997). Myosin II-independent processes in mitotic cells of *Dictyostelium discoideum*: redistribution of the nuclei, re-arrangement of the actin system and formation of the cleavage furrow. J. Cell Sci. *110*(Pt 2), 123–137.

Olazabal, I. M., Caron, E., May, R. C., Schilling, K., Knecht, D. A., and Machesky, L. M. (2002). Rho-kinase and myosin-II control phagocytic cup formation during CR, but not FcgammaR, phagocytosis. Curr. Biol. *12*, 1413–1418.

Pellegrin, S., and Mellor, H. (2007). Actin stress fibres. J. Cell Sci. *120*, 3491–3499.

Pollard, T. D., and Borisy, G. G. (2003). Cellular motility driven by assembly and disassembly of actin filaments. Cell *112*, 453–465.

Ridley, A. J., Schwartz, M. A., Burridge, K., Firtel, R. A., Ginsberg, M. H., Borisy, G., Parsons, J. T., and Horwitz, A. R. (2003). Cell migration: integrating signals from front to back. Science *302*, 1704–1709.

Salmon, W. C., Adams, M. C., and Waterman-Storer, C. M. (2002). Dual-wavelength fluorescent speckle microscopy reveals coupling of microtubule and actin movements in migrating cells. J. Cell Biol. *158*, 31–37.

Schaefer, A. W., Kabir, N., and Forscher, P. (2002). Filopodia and actin arcs guide the assembly and transport of two populations of microtubules with unique dynamic parameters in neuronal growth cones. J. Cell Biol. *158*, 139–152.

Schaub, S., Bohnet, S., Laurent, V. M., Meister, J. J., and Verkhovsky, A. B. (2007). Comparative maps of motion and assembly of filamentous actin and myosin II in migrating cells. Mol. Biol. Cell *18*, 3723–3732.

Sheetz, M. P. (1994). Cell migration by graded attachment to substrates and contraction. Semin. Cell Biol. *5*, 149–155.

Sheetz, M. P., Felsenfeld, D., Galbraith, C. G., and Choquet, D. (1999). Cell migration as a five-step cycle. Biochem. Soc. Symp. *65*, 233–243.

Signoret, N., Hewlett, L., Wavre, S., Pelchen-Matthews, A., Oppermann, M., and Marsh, M. (2005). Agonist-induced endocytosis of CC chemokine receptor 5 is clathrin dependent. Mol. Biol. Cell *16*, 902–917.

Small, J. V. (1995). Getting the actin filaments straight: nucleation-release or treadmilling? Trends Cell Biol. *5*, 52–55.

Small, J. V., and Resch, G. P. (2005). The comings and goings of actin: coupling protrusion and retraction in cell motility. Curr. Opin. Cell Biol. *17*, 517–523.

Small, J. V., Rottner, K., Kaverina, I., and Anderson, K. I. (1998). Assembling an actin cytoskeleton for cell attachment and movement. Biochim. Biophys. Acta *1404*, 271–281.

Straight, A. F., Cheung, A., Limouze, J., Chen, I., Westwood, N. J., Sellers, J. R., and Mitchison, T. J. (2003). Dissecting temporal and spatial control of cytokinesis with a myosin II inhibitor. Science *299*, 1743–1747.

Svitkina, T. M., Bulanova, E. A., Chaga, O. Y., Vignjevic, D. M., Kojima, S., Vasiliev, J. M., and Borisy, G. G. (2003). Mechanism of filopodia initiation by reorganization of a dendritic network. J. Cell Biol. *160*, 409–421.

Svitkina, T. M., Verkhovsky, A. B., McQuade, K. M., and Borisy, G. G. (1997). Analysis of the actin-myosin II system in fish epidermal keratocytes: mechanism of cell body translocation. J. Cell Biol. *139*, 397–415.

Swailes, N. T., Knight, P. J., and Peckham, M. (2004). Actin filament organization in aligned prefusion myoblasts. J. Anat. *205*, 381–391.

Tanner, G. A., Sandoval, R. M., Molitoris, B. A., Bamburg, J. R., and Ashworth, S. L. (2005). Micropuncture gene delivery and intravital two-photon visualization of protein expression in rat kidney. Am. J. Physiol. Renal Physiol. *289*, F638–F643.

Urven, L. E., Yabe, T., and Pelegri, F. (2006). A role for non-muscle myosin II function in furrow maturation in the early zebrafish embryo. J. Cell Sci. *119*, 4342–4352.

Vallotton, P., Danuser, G., Bohnet, S., Meister, J. J., and Verkhovsky, A. B. (2005). Tracking retrograde flow in keratocytes: news from the front. Mol. Biol. Cell *16*, 1223–1231.

Vallotton, P., Gupton, S. L., Waterman-Storer, C. M., and Danuser, G. (2004). Simultaneous mapping of filamentous actin flow and turnover in migrating cells by quantitative fluorescent speckle microscopy. Proc. Natl. Acad. Sci. USA *101*, 9660–9665.

Verkhovsky, A. B., Svitkina, T. M., and Borisy, G. G. (1995). Myosin II filament assemblies in the active lamella of fibroblasts: their morphogenesis and role in the formation of actin filament bundles. J. Cell Biol. *131*, 989–1002.

Verkhovsky, A. B., Svitkina, T. M., and Borisy, G. G. (1999). Network contraction model for cell translocation and retrograde flow. Biochem. Soc. Symp. *65*, 207–222.

Zhou, M., and Wang, Y. L. (2008). Distinct pathways for the early recruitment of myosin II and actin to the cytokinetic furrow. Mol. Biol. Cell *19*, 318–326.